LOW-DIMENSIONAL AND DISORDERED SYSTEMS

Noninteracting electrons in one-dimensional systems

V. F. Gantmakher*

Institute of Solid State Physics, Russian Academy of Sciences, Chernogolovka, Russia
(Submitted September 7, 2004)
Fiz. Nizk. Temp. **31**, 436–444 (March–April 2005)

The theoretical fundamentals for describing the behavior of noninteracting electrons in one-dimensional systems are presented: the transport characteristics of an ideal wire connecting two thermostats; a description of elastic scattering by a chaotic sequence of barriers using Landauer's formula; gigantic chaotic oscillations of the resistance; localization; and, the influence of correlations in a random potential on the localization. © *2005 American Institute of Physics.* [DOI: 10.1063/1.1884437]

The purpose of the present brief review is to present the theoretical fundamentals for describing one-dimensional systems of noninteracting electrons and illustrating their behavior on the basis of known experiments. The number of one-dimensional objects which are available to experimentalists has increased substantially in the last few years. Examples are organic metals,[1] semiconductor nanowires,[2] carbon nanotubes,[3] and even real, short chains of metal atoms.[4] This has drawn more people into working with such objects and has made it necessary to provide them with a quite rigorous introduction to this problem.

The criterion for one-dimensionality is associated with the structure of the electron spectrum of free electrons with wave functions $\exp(i\mathbf{k}\cdot\mathbf{r})$ and the appropriate geometry of the region of their existence

$$\varepsilon=\hbar^2k_\parallel^2/2m+\varepsilon_\perp(i),\quad i=1,2,\ldots. \tag{1}$$

Here $k_\parallel$ is the wave number in the direction in which the electron motion is unbounded; $\varepsilon_\perp$ is the size-quantized part of the energy associated with motion in bounded directions; i enumerates the size-quantized subbands. A system is one-dimensional ($1D$) if all electrons fit into the bottom subband. For a degenerate electronic system the criterion is

$$\varepsilon_F<\Delta_s,\quad \Delta_s\equiv\varepsilon_\perp(i=2)-\varepsilon_\perp(i=1). \tag{2}$$

If several size-quantized subbands lie below the Fermi level, then the system is quasi-one-dimensional.

Generally speaking, interelectronic interactions have a large effect on the behavior of electrons in $1D$ systems. Concepts such as the Luttinger liquid and a wave of charge or spin density arose precisely from studying $1D$ systems. Taking account of interactions greatly complicates the analysis of the experimental data and often makes the analysis ambiguous. Consequently, it is helpful to have as a starting basis a clear picture of the behavior of noninteracting electrons in $1D$ systems. This picture is presented in the present review. First, it is postulated that the wave function of an electron is a plane wave $\exp(i\mathbf{k}\cdot\mathbf{r})$ and interference processes in the wave field formed as a result of the propagation and scattering of this wave in a one-dimensional potential are examined.

According to the Peierls theorem a $1D$ system with an ideal periodic potential is unstable with respect to the appearance of a new period and a wave of charge density,[5] and arbitrarily weak disorder in a one-dimensional medium results in localization.[6] Nonetheless, conduction in a $1D$ system of noninteracting electrons is possible because of temperature, the finite length of the $1D$ system, and correlations in a random potential.

1. IDEAL WIRE

We consider first an ideal wire with no scattering, even elastic scattering. Let an ideal wire of length Λ connect two reservoirs to which a potential difference V is applied. Then any electron entering the wire on one side leaves the wire on the other side with probability one. In addition, let the diameter of the wire be so small that the spectrum (1) of the wire below the Fermi level ε_F contains a finite number $\nu=2N_s$ of size-quantized subbands (they are also called channels; in the absence of a magnetic field, for every $i\leqslant N_s$ there exist two channels with different spin directions):

$$\varepsilon_\perp(i)<\varepsilon_F\ \text{ for }\ i=1,2,\ldots,N_s. \tag{3}$$

If $N_s=1$, then the $1D$ system is said to be a single-channel system (taking the spin of the system into account it could also be called a two-channel system), and for $N_s>1$ it is called a multichannel system. Since the wire is ideal, the channels inside the wire are independent of one another and do not exchange electrons. The electron density n_i in channel i, the longitudinal velocity of the electrons v_i, and the density of states g_i at the Fermi level are related by the relations

$$v_i=\hbar^{-1}(\partial\varepsilon/\partial k)_{\varepsilon=\varepsilon_i},\quad g_i=(\partial n_i/\partial\varepsilon)_{\varepsilon=\varepsilon_i}=1/2\pi\hbar v_i,$$

$$\varepsilon_i=\varepsilon_F-\varepsilon_\perp(i),\quad 2\sum_{i=1}^{N_s}n_i=n. \tag{4}$$

The presence of a potential difference V between the reservoirs means that because of the difference in the electron density $\delta n_i = g_i eV$ there is a difference between the electron fluxes entering the channel i from the right- and left-hand sides. In the expression for the current the concrete parameters of the channel appearing in the relations (4) cancel, so that the current J_i in the channel is independent of the index i and equals

$$J_i = ev_i \delta n_i = (e^2/2\pi\hbar)V. \tag{5}$$

The conductance $y_{\rm id} = J/V$ and the resistance $\rho_{\rm id} = 1/y_{\rm id}$ of such a wire are determined by the total current $J = \Sigma_1^\nu J_i$ and equal

$$y_{\rm id} = (e^2/2\pi\hbar)\nu, \quad \rho_{\rm id} = (2\pi\hbar/e^2)(1/\nu). \tag{6}$$

The index here underscores the fact that Eq. (6) refers to an ideal wire.

The result (6) is remarkable in several respects. In the first place it has been found that in a $1D$ system, even a multichannel system, dissipation occurs even in the absence of scattering. In the second place, however surprisingly, the resistivity $\rho_{\rm id}$ of the wire is independent of its length and is determined only by the quantization of the electronic spectrum. Both of these circumstances are a manifestation of the principle of nonlocality. The electrons acquire energy in locations where a field is present, i.e. in or at the edges of the wire, and give up energy when they are thermalized in a reservoir, i.e. far from the wire.

It is no accident that we do not specify more accurately where the electric field is concentrated. The arguments which have led to Eq. (6) do not predetermine the distribution of the electric field along the wire. Additional considerations are required to determine this distribution. Ordinarily, it is found that the field is distributed nonuniformly along a channel and concentrated predominantly near its ends. In this respect an interesting example are edge channels which are formed along the edge of a sample between the contacts in the presence of a quantum Hall effect. In a strong magnetic field perpendicular to the plane of a two-dimensional electron gas all electrons colliding with and reflected from the surface necessarily collide with the surface again in the next turn of their cyclotron motion. The direction of their displacement along the surface in the time between two collisions with the surface is determined by the sign of the vector product of the field and the normal to the region of the two-dimensional gas and is independent of the angle of incidence and the angle of reflection of the electron. The current along the surface is described using the concept of a one-dimensional channel, which is ideal because of the absence of backscattering. The tangential electric field along the edge of a sample, i.e., along a $1D$ channel, is everywhere zero in the presence of a quantum effect of the field, and the entire voltage drop is concentrated at the boundary with one of the contacts.[7]

It would appear that the assertion that the resistance of a wire is independent of its length contradicts a simple argument. Imagine an ideal wire to be divided into two parts which are connected in series. If the resistance is $\rho_{\rm id}$ in each part, then the total resistance should be $2\rho_{\rm id}$. But it is not enough to simply divide the wire into two parts. In order for both parts to be independent resistances an additional reservoir-thermostat must be inserted between them, and this reservoir-thermostat would make the electronic waves passing through it incoherent. If the temperature of the wire is different from absolute zero, $T \neq 0$, so that there exists a finite length $L_\varphi < \infty$ over which an inelastic collision and phase interference of the electronic wave occur, then such thermostats appear automatically at distances L_φ from one another.

Thus there is an upper bound on the length of an ideal wire, $\Lambda < L_\varphi$. The lower bound is actually the diameter of the wire. This is evident from an analysis of a Sharvin contact,[8] where an insulating flat diaphragm with an opening with area S divides two three-dimensional metal half-spaces, one of which is an "ideal" crystal in the sense that the mean-free path length there is $l \gg \sqrt{S}$. The resistence of such a contact is

$$R \approx \frac{\hbar k_F}{ne^2 S} \approx \frac{\hbar}{e^2}\left(\frac{\hbar^2/mS}{\varepsilon_F}\right), \tag{7}$$

where n, m, $k_F = (3\pi^2 n)^{1/3}$ and $\varepsilon_F = \hbar^2 k_F^2/2m$ are the concentration, mass, Fermi momentum, and Fermi energy, respectively, of the electron gas in an ideal half-space, and the $\approx$ sign appearing instead of an $=$ sign signifies that numerical coefficients are dropped in the expression. It is easy to verify that the expression (7) is identical in structure to the expression (6) for $\rho_{\rm id}$, and the numerator in the fraction in parentheses in Eq. (7) is the characteristic splitting $\varepsilon_\perp$ between the size-quantized subbands. It is easy to verify for a square opening that this distance is indeed proportional to S^{-1}.

Since an experimental channel can be very short, Eq. (6) can be checked experimentally. Figure 1 shows the results of measurements of the conductivity of a narrow channel under a split gap connecting two regions of a $2D$ electron gas in a GaAs–Al$_x$Ga$_{1-x}$As heterostructure.[9] As the blocking voltage V_g on the gate increases, the depleted region expands somewhat because it extends slightly beyond the edge of the gate. As one can see in the inset in Fig. 1, the conducting channel narrows, which means that the number of channels N_s decreases. The short length of the channel makes it possible to obtain a ballistic regime, i.e. a no-scattering regime, in it. In

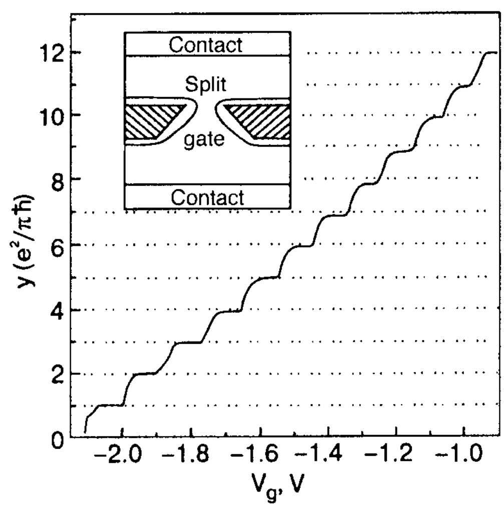

FIG. 1. Conductance y of a ballistic contact between $2D$ regions of a GaAs-Al$_x$Ga$_{1-x}$As heterostructure as a function of the gate voltage regulating the width of the contact.[9] Inset: layout of the measuring cell.

the structure shown in Fig. 1 the electron density is 3.56×10^{11} cm^{-2}, the mean-free path length at 0.6 K is about 8.5 μm, and the characteristic dimensions of the channel are of the order of 0.25 μm.

It is evident in the inset in Fig. 1 that the measurement is performed by a two-contact scheme, so that the measured resistance $R_{\rm meas}$ contains the resistance $R_{\rm cont}$ of the contacts and the resistance of the adjoining wide sections of the $2D$ layer. The conductance, which is of interest to us, is $y \equiv \rho^{-1} = (R_{\rm meas} - R_{\rm cont})^{-1}$. The resistance $R_{\rm cont}$ was assumed to be 4.35 kΩ, so that it corresponds approximately to the results of independent measurements. After this quantity is subtracted the function $y(V_g)$ becomes a sequence of steps of the same height

$$\Delta y_{\rm id} = (e^2/2\pi\hbar)\Delta\nu = e^2/\pi\hbar, \tag{8}$$

in complete agreement with Eq. (6).

2. ELASTIC SCATTERERS

We now assume the wire to be nonideal and, for simplicity, a one-channel system. Let elastic scatterers be present in the hatched section of the wire (Fig. 2). There is no need to specify their relative arrangement more accurately—we shall consider the entire hatched region to be a single scattering object. In quantum mechanics, it is characterized in the one-dimensional case by complex reflection r and transmission t coefficients, which couple the amplitudes of the reflected and transmitted waves with the amplitude of the incident wave. Electronic fluxes $j_{\rm in}/e$ and $j'_{\rm in}/e$ are incident from the left and right on the hatched region. Each electron is reflected with probability $\mathcal{R} = |r|^2$ and is transmitted with probability $\mathcal{T} = |t|^2$.

$$\mathcal{R} = j_r/j_{\rm in} = j'_r/j'_{\rm in}, \quad \mathcal{T} = j_t/j_{\rm in} = j'_t/j'_{\rm in}, \tag{9}$$
$$\mathcal{R} + \mathcal{T} = 1.$$

If the voltage drop on the hatched region is zero, then the total electron flux in the wire is also zero. In the presence of a potential difference δV, a density difference $\delta n = g e \delta V$ appears at the boundaries of the region. In one-dimensional systems all electrons move along the wire and therefore belong to one of the fluxes appearing in Eqs. (9). This makes it possible to relate δn with the electron densities in the fluxes and express δV in terms of the current:

$$\delta V = \frac{\delta n}{ge} = \frac{j_{\rm in} + j_r + j'_t}{e^2 g v} - \frac{j'_{\rm in} + j'_r + j_t}{e^2 g v} = \frac{2\mathcal{R}(j_{\rm in} - j'_{\rm in})}{e^2 g v}. \tag{10}$$

Here g and v are the density of states and the modulus of the velocity of the electrons at the Fermi level. Since the total current J is

$$J = j_{\rm in} - j_r - j'_t = j'_{\rm in} - j'_r - j_t = \mathcal{T}(j_{\rm in} - j'_{\rm in}), \tag{11}$$

the ratio $J/\delta V$ makes it possible to represent the conductance $y_{\rm imp} = J/\delta V$ and the resistance $\rho_{\rm imp} = y_{\rm imp}^{-1}$ of the hatched region in the form

$$y_{\rm imp} = \frac{e^2}{2\pi\hbar}\frac{\mathcal{T}}{\mathcal{R}} = \frac{e^2}{2\pi\hbar}\frac{\mathcal{T}}{1-\mathcal{T}},$$

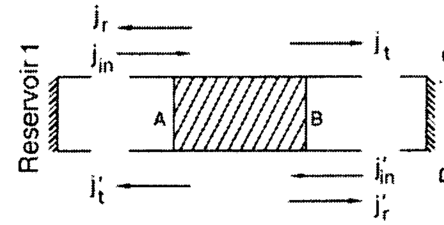

FIG. 2. One-dimensional conductor connecting two reservoirs and consisting of two ideal sections along the edges and the scattering section AB at the center.

$$\rho_{\rm imp} = \frac{2\pi\hbar}{e^2}\frac{\mathcal{R}}{\mathcal{T}} = \frac{2\pi\hbar}{e^2}\frac{\mathcal{R}}{1-\mathcal{R}}. \tag{12}$$

The idea of representing elastic scattering centers as potential barriers in the path of propagating waves and expressing the transport characteristics of the system in terms of the reflection and transmission coefficients of the wave for these barriers was first advanced by Landauer.[10] Consequently, the corresponding formulas, specifically, the expression for the conductance (12), are named after Landauer. In principle Landauer's technique is applicable to systems of any dimension, but it is especially convenient and often used for $1D$ systems.

Landauer's formula in the form (12) was derived under the assumption that the potential difference is applied directly to the scattering region between the points A and B in Fig. 2. This is why the conductance (12) with weak scattering, $\mathcal{T} \sim 1$, $\mathcal{R} \ll 1$, can be greater than the conductance (6) of a system with no scatterers. If the potential difference in the system in Fig. 2 is applied to the reservoirs, then the resistances of the ideal wire and the scattering region are connected in series and the conductance of the entire system is

$$y^{-1} = y_{\rm id}^{-1} + y_{\rm imp}^{-1} \equiv \rho_{\rm id} + \rho_{\rm imp} = \frac{2\pi\hbar}{e^2}\left(1 + \frac{\mathcal{R}}{\mathcal{T}}\right),$$

$$y = \frac{e^2}{2\pi\hbar}\mathcal{T}. \tag{13}$$

Now, the conductance $y \to y_{\rm id}$ as $\mathcal{T} \to 1$, as should be. The expression (13) for y can also be obtained directly by applying a potential difference to the reservoirs, writing the electron flux from one reservoir into another, and taking account of single scattering (compare with the derivation of Eq. (6)). This means that adding the resistances in accordance with Ohm's law in the arguments for Eq. (13) was justified. How-

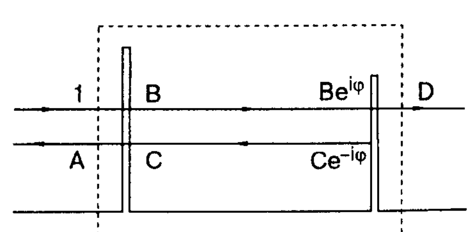

FIG. 3. Scattering section in a $1D$ conductor consisting of two barriers. The complex amplitudes $A, \ldots, D$ of the waves arriving at and leaving both barriers are normalized to the initial arriving wave, indicated by the number 1.

ever, this is by no means always the case for one-dimensional systems because the incident and reflected waves interfere with one another.

We shall now consider two successive barriers in a single-channel one-dimensional conductor (Fig. 3) and we shall express in terms of the parameters $\mathcal{T}_1$, $\mathcal{R}_1$, $\mathcal{T}_2$, and $\mathcal{R}_2$ of the initial barriers the parameters $\mathcal{T}$ and $\mathcal{R}=1-\mathcal{T}$ of the compound scattering object formed. If a wave with amplitude 1 is incident on the barrier from the left, then the stationary wave field formed will contain four additional waves: the reflected wave A, the transmitted wave D, and two oppositely propagating waves B and C between the barriers ($A, \ldots, D$ are the complex amplitudes of the waves). Expressing the amplitudes of the waves moving to the right and left of each of the barriers in terms of the amplitudes of the incident waves, we obtain four equations:

$$A=r_1+Ct_1, \quad B=t_1+Cr_1, \quad Ce^{-i\varphi}=Be^{i\varphi}r_2,$$

$$D=Be^{i\varphi}t_2. \tag{14}$$

Here the fact that the reflection coefficient of the barrier is independent of the side from which the wave is incident is taken into account, $r_1=r_1'$; the factors $\exp(\pm i\varphi)$ take account of the phase shift of the wave over the distance from one barrier to the other. From Eqs. (14) follows

$$D=\frac{e^{i\varphi}t_1t_2}{1-e^{2i\varphi}r_1r_2},$$

$$\mathcal{T}=|D|^2=\frac{\mathcal{T}_1\mathcal{T}_2}{1+\mathcal{R}_1\mathcal{R}_2-2\sqrt{\mathcal{R}_1\mathcal{R}_2}\cos\theta}, \tag{15}$$

where $\theta=2\varphi+\arg(r_1r_2)$. The conductance Y_2 of the a compound "two-barrier" scatterer, marked in Fig. 3 by the dotted line, is

$$Y_2=\frac{e^2}{2\pi\hbar}\frac{\mathcal{T}}{1-\mathcal{T}}=\frac{e^2}{2\pi\hbar}\frac{\mathcal{T}_1\mathcal{T}_2}{\mathcal{R}_1+\mathcal{R}_2-2\sqrt{\mathcal{R}_1\mathcal{R}_2}\cos\theta}. \tag{16}$$

If a compound "double-barrier" scatterer consists of two identical barriers, $r_1=r_2=r'$, $t_1=t_2=t'$, $\mathcal{R}_1=\mathcal{R}_2=\mathcal{R}'$, and so on, then

$$Y_2=\frac{e^2}{2\pi\hbar}\frac{(\mathcal{T}')^2}{4\mathcal{R}'\sin^2\theta/2},$$

$$\theta/2=\varphi+\arg(r')=kl+\arg(r'), \tag{17}$$

where k is the wave number and l is the distance between the barriers.

The conductance (16) depends not only on the parameters of the two initial barriers. Through the angle θ it also depends on the distance between the barriers. Ultimately, we are interested in a $1D$ conductor with a large number of randomly positioned barriers. Therefore we can average over all possible distances between them, making the assumption that the angle θ assumes any value from 0 to 2π with equal probability. Such averaging is not entirely correct, but it makes it possible to follow the trends arising as the length of the chain of one-dimensional barriers increases (see Ref. 11 and also the original work[12] for a more detailed discussion). The average conductance $\overline{Y_2}$ of a system of two barriers follows from the average value $\overline{\cos\theta}=0$:

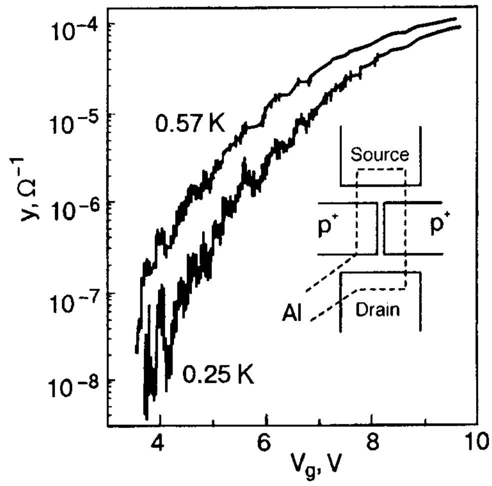

FIG. 4 Conductance y of a long quasi-one-dimensional channel in a field-effect transistor, fabricated on the surface of n-Si, in the accumulating layer regime as a function of the gate voltage V_g.[13] The width of the channel can vary from 0 up to the maximum value $\sim 1\ \mu$m, set by the construction (see the scheme shown in the inset), using voltages on the control electrodes p^+ and on the gate.

$$\overline{Y_2}=\frac{e^2}{2\pi\hbar}\frac{\mathcal{T}_1\mathcal{T}_2}{\mathcal{R}_1+\mathcal{R}_2}=\frac{e^2}{2\pi\hbar}\frac{(1-\mathcal{R}_1)(1-\mathcal{R}_2)}{\mathcal{R}_1+\mathcal{R}_2}. \tag{18}$$

For comparison we shall give the classical expression for a sum of two successive resistances $\rho_1=y_1^{-1}$ and $\rho_2=y_2^{-1}$:

$$Y_2^{(\mathrm{cl})}=(y_1^{-1}+y_2^{-1})^{-1}\equiv(\rho_1+\rho_2)^{-1}$$
$$=\frac{e^2}{2\pi\hbar}\left(\frac{\mathcal{R}_1}{1-\mathcal{R}_1}+\frac{\mathcal{R}_2}{1-\mathcal{R}_2}\right)^{-1}$$
$$=\frac{e^2}{2\pi\hbar}\frac{(1-\mathcal{R}_1)(1-\mathcal{R}_2)}{\mathcal{R}_1+\mathcal{R}_2-2\mathcal{R}_1\mathcal{R}_2} \tag{19}$$

In Eq. (19) there is an extra, compared with Eq. (18), term in the denominator, proportional to the product of the transmission coefficients $\mathcal{R}_1\mathcal{R}_2$ for two barriers.

3. GIGANTIC OSCILLATIONS OF THE RESISTANCE

We shall discuss one other feature of transport in $1D$ systems. Figure 4 shows the transport characteristics of a quasi-one-dimensional system fabricated on the basis of an accumulating layer in a field-effect transistor on a n-Si surface.[13] At low temperatures a noise-like component with very large amplitude appears in the dependence of the conductance y on the gate voltage V_g. This is not real noise. The signal does not depend on the time, and if the sample is not heated to room temperature, then in a repeated experiment the curve $y(V_g)$ will be reproduced right down to the smallest details. It is evident that at low temperatures and gate voltages V_g allowing for a narrow channel and low carrier concentration, the conductance undergoes as a function of V_g chaotic narrow oscillations whose total range increases with decreasing temperature. For a different sample, and even for the same sample, with repeated cooling from room temperature the detailed structure of the oscillations is different with the same overall pattern of evolution of oscillations with a change in the temperature and voltage V_g.

The fundamental reason for the chaotic oscillations is one-dimensionality. All defects in a wire are connected in series, and the current lines cannot circumvent any of them. Consequently, switching off one strongly scattering defect can strongly influence the total resistance. The question is how a change in V_g that changes the concentration and Fermi energy ε_F of the carriers can switch on, switch off, or change the effectiveness of individual defects.

Let us return to the expression (17) for the conductance Y_2 of a symmetric "double-barrier" scatterer. In the discussion above we averaged the expression (16) over $\cos\theta$ on the basis that there is a spread in the values of the distances l_i between the barriers. But the angle $\varphi = kl_i$ appearing in θ depends not only on l_i but also on the wave number k, i.e., on the energy ε_F of the scattering electron. For one specific scattering pair of barriers with a fixed value of l_i it follows from Eq. (17) that R_2 assumes values from 0 to 4ρ,

$$0 \leqslant R_2 \leqslant 4\rho, \tag{20}$$

depending on the energy of the incident electron. Here it should be recalled that the transport properties of a $1D$ system are determined precisely by the electrons from a neighborhood of ε_F because the opposite electron fluxes with lower energies compensate one another. We mentioned above that there are problems with averaging the expression for the resistance (16). They are due precisely to the wide range (20) of variation of R_2.

The space between two barriers is a potential well. In this well, generally speaking, there is a collection of levels ε_i whose widths are due to the transmittances t_1 and t_2 of the barriers. As the electron energy ε_F shifts relative to the system of levels in this well the tunneling probability oscillates, reaching a maximum at resonance $\varepsilon_F = \varepsilon_i$. Consequently, the gigantic chaotic oscillations of the resistance can be described theoretically precisely in terms of resonance tunneling.[14]

The model of localized states in $1D$ systems employs the idea of electronic levels inside composite scatterers. At sufficiently low temperatures reflections from distant barriers

$$1 \ll N \ll L_\varphi / l \tag{21}$$

remain coherent. Consequently, according to the relation (25) presented below, these reflections for sufficiently large L_φ compensate the barrier transmittances of t_1 and t_2 and make the state between them localized. Hopping conductivity should be expected under these conditions. Indeed, Fig. 5 displays measurements of the temperature dependence of the conductance which were performed at several minima of the curve presented in Fig. 4. It is evident that for measurements on the left-hand side of the plot in Fig. 4, for lower values of V_g when the conductance is small, the oscillations are large and there is every reason to regard the channel to be one-dimensional, the points follow well the functional dependence

$$y = y_0 \exp[-(T_M/T)^{1/2}] \tag{22}$$

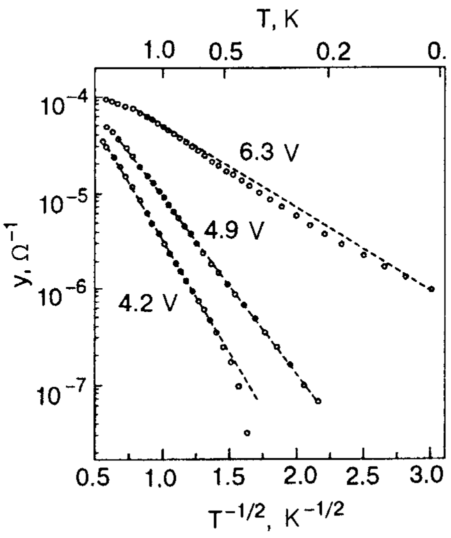

FIG. 5. Temperature dependences at the minima of the conductance of a channel of a field-effect transistor for three different values of the gate voltage V_g.[13]

in complete agreement with Mott's formula for the temperature dependence of hopping conductivity with variable hopping distance:

$$\rho = \rho_0 \exp\left(\frac{T_M}{T}\right)^{1/(d+1)}, \quad T_M \approx (g_\mu \xi^d)^{-1}, \tag{23}$$

where d is the dimension of the space and ξ is the decay length of localized states.

For large values of V_g the channel expands and gradually converts into a two-dimensional channel. The conductance increases, and the amplitude of the chaotic oscillations decreases. The experimental points of the function $\log y(T^{-1/2})$ obtained with gate voltage $V_g = 6.3$ V deviate in Fig. 5 from a straight line, but they rectify in the $(\log y, T^{-1/3})$ plane, once again in complete agreement with Eq. (23).

4. LOCALIZATION

Let us consider a long chain of identical, weakly scattering barriers, $\mathcal{R}' \ll 1$ and $\mathcal{T}' \sim 1$, located at random distances l_i from one another and each having a small resistance $\rho' = (2\pi\hbar/e^2)(\mathcal{R}'/\mathcal{T}') \ll 2\pi\hbar/e^2$ (the average distance between the barriers $l = \overline{l_i}$ is the elastic mean-free path length). We shall calculate the resistance $R_N = Y_N^{-1} = (2\pi\hbar/e^2) \times (\mathcal{R}_N/\mathcal{T}_N)$ of a compound scattering object consisting of N barriers using a recurrence relation following from Eq. (18):

$$\frac{\mathcal{R}_N}{\mathcal{T}_N} = \frac{\mathcal{R}_{N-1} + \mathcal{R}'}{\mathcal{T}_{N-1}\mathcal{T}'}. \tag{24}$$

As long as the number of barriers N is small, so that $N\rho' \ll 2\pi\hbar/e^2$, the resistance R_N increases linearly: $R_N \approx N\rho \propto N$. The reflection probability $\mathcal{R}_N$ also increases almost linearly. But $\mathcal{R}_N$ cannot exceed 1. Consequently, at some value of N we can set $\mathcal{R}_N \approx \mathcal{R}_{N-1} \approx 1$ in Eq. (24), whence it immediately follows that

$$\mathcal{T}_N \approx \mathcal{T}_{N-1}\mathcal{T}', \quad \mathcal{T}_N \to s(\mathcal{T}')^N = s e^{\alpha N} \text{ as } N \to \infty,$$
$$(s = \text{const}, \quad \alpha = \ln \mathcal{T}' < 0). \tag{25}$$

The exponential decrease of the transmitted-wave intensity $\mathcal{T}_N$ with increasing N is a demonstration of $1D$ localization for a specific example.

5. ROLE OF CORRELATIONS IN A RANDOM POTENTIAL

The general assertion of Ref. 16 that $1D$ localization occurs in a random potential and the illustration (25) of this assertion for a specific model assumed that there are no correlations. However, localization may not occur if the chaotic one-dimensional potential is not completely random but contains correlators. To show this we return to Eq. (17) for the conductance Y_2 of the symmetric "double-barrier" scatterer shown in Fig. 3. It follows form this formula that there exists a wave number $k_0=-\arg(r')/l$ for which the barrier is completely transparent to the incident wave and there is no reflected wave $\mathcal{R}_2'=0$. If in our model (24)–(25) the isolated barriers are replaced with double barriers (17), then an electron with energy $\varepsilon_0=\hbar^2k_0^2/2m$ will be delocalized.

This idea was elaborated in the so-called dimer model.[15] This model uses not one-dimensional barriers but rather a one-dimensional chain of periodically arranged potential wells. The chain consists of two types of wells with energy levels E_a and E_b. The wells are distributed along the odd lattice sites completely randomly, without any correlations, and each even site contains a well of the same type as the odd site to the left of it. This means that identical wells occur in pairs, whence the name of the model (Fig. 6a). If the distance between the wells is a, then the lattice obtained can be represented as a sum of two random but identical *sublattices*, shifted by a with respect to one another, both with period $2a$ and an entirely random distribution of wells over the sites.

We shall assume that pairs with energy E_a belong to the main lattice and pairs with energy E_b are defects. As we have already seen, in this model localized states can exist for certain specified values of the energy. Now, it is necessary to formulate the condition under which electrons with this energy can propagate in the main lattice.

Consider one dimer defect consisting of two wells with energy E_b in an ideal lattice consisting of E_a wells (Fig. 6b). Let the overlap integral between neighboring wells be J. Then bands with a quasicontinuous distribution of levels $\varepsilon=E_a-2J\cos ka$ are formed to the right and left of a defect. If

$$|E_a-E_b|<2J, \tag{26}$$

then the unperturbed energy level E_b of a defect falls within the band and a distinguished value $k=k_0$, $\cos k_0=-2J/(E_a-E_b)$, for which the reflection probability of a defect $\mathcal{R}=0$, appears in the band.

In the dimer model correlations exist only between nearest neighbors. For such correlations delocalized states arise only for discrete values of the energy. To obtain a band of delocalized states distant correlations must be used, retaining in so doing an element of randomness. An algorithm for constructing such a potential was proposed in Refs. 16 and 17. Here we present only a specific example of such an algorithm, constructed to perform an experimental check by means of microwave simulation.

Microwave simulation of localization processes is possible because the time-dependent Schrödinger equation

$$i\hbar\frac{\partial\Psi}{\partial t}=-\frac{\hbar^2}{2m}\Delta\Psi+U\Psi \tag{27}$$

and the classical wave equation

$$\frac{1}{c^2}\frac{\partial^2\Psi}{\partial t^2}=\Delta\Psi-U\Psi \tag{28}$$

(c is the speed of light) have much in common.[8] The substitution $\Psi=e^{-i\omega t}\psi$ reduces both equations to

$$(\Delta-U+k^2)\Psi=0 \tag{29}$$

the only difference being that for the Schrödinger equation

$$\omega=(\hbar/2m)k^2, \tag{30}$$

and for the wave equation

$$\omega=ck. \tag{31}$$

As an example of microwave simulation we present the experiment of Ref. 19 where the transmission coefficient of a long waveguide was measured as a function of frequency for an electromagnetic wave in the microwave range. The waveguide scheme is shown in Fig. 7. The working frequency range was chosen to lie inside the frequency range where the waveguide is in a single-mode regime: $7.5\,\text{GHz}=c/2a<\omega/2\pi<c/a=15$ GHz, where a is the large dimension of the transverse cross section of the waveguide.

To simulate the random potential $N=100$ scatterering pins are inserted at equal distances along the waveguide. Using micrometric screws the pins can be inserted to different depths u_n, where $1\leqslant n\leqslant N$. The depth is set using the formula

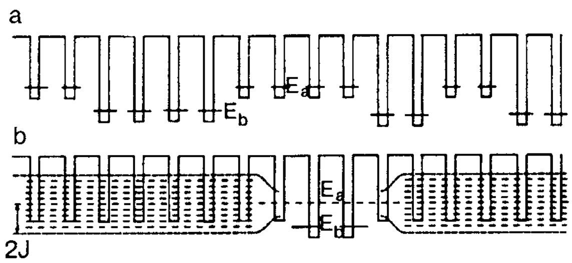

FIG. 6. Dimer model of a one-dimensional random potential. The changes occurring in the positions of the levels as a result of the overlapping of the wells are not shown (a). The electron levels in a one-dimensional lattice with one dimer defect (b).

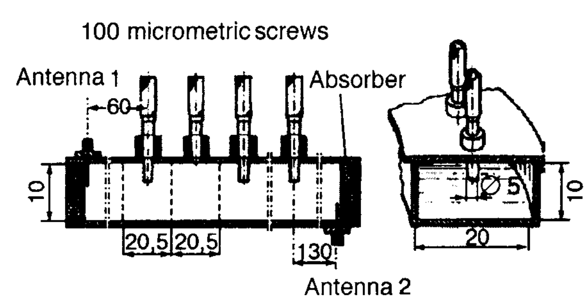

FIG. 7. Schematic diagram of a single-mode waveguide with 100 scatterers, in which the transmission coefficient t for an electromagnetic wave was measured as a function of the frequency.[19] All dimensions are given in mm.

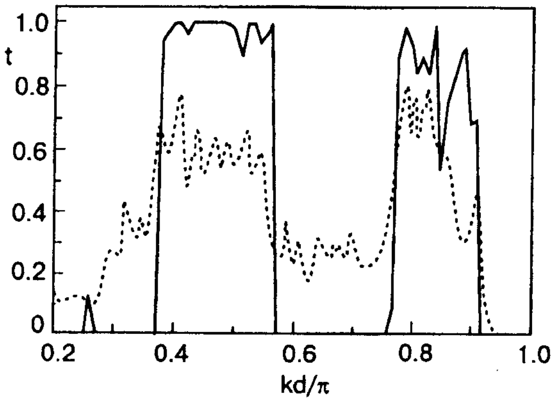

FIG. 8. Transmission coefficient t of a wave in a one-dimensional channel in the presence of periodically arranged random scatterers which are correlated by means of a specially chosen correlation function.[19] Solid line—numerical experiment with $N=10^4$ scatterers; dashed line—microwave experiment with $N=100$ scatterers, averaged over five different realizations. The correlation function is the same.

$$u_n=\sqrt{\overline{u_n^2}}\sum_{m=-\infty}^{\infty}\beta_m Z_{n+m},$$

$$\beta_m=\frac{2}{\pi}\int_0^{\pi/2}\sqrt{\varphi(\mu)}\cos(2m\mu)d\mu. \tag{32}$$

Here Z_{n+m} are random numbers from -1 to $+1$. They introduce an element of randomness into the potential. The correlations between all u_n are provided by the factors β_m, determined in terms of the function $\varphi(\mu)$. The latter function is chosen using a special mathematical algorithm depending on the type of transmission spectrum required for the one-dimensional system. An example of the implementation of such a program is shown in Fig. 8. This was used to choose a function $\varphi(\mu)$ for which two transmission bands should arise inside the working range. The solid line in the figure shows the transmission coefficient, determined in a numerical experiment, of a waveguide with a one-dimensional sequence of $N=10^4$ scatterers chosen in accordance with Eq. (32) using the prescribed function $\varphi(\mu)$. The dashed line shows the result of a real microwave experiment with a sequence of $N=100$ scatterers averaged over five different realizations.

6. CONCLUSIONS

These are the basic fundamentals of the behavior of noninteracting electrons in one-dimensional systems with a random potential. They should be kept in mind when discussing any experiments in such systems, even if the interelectronic interactions play the main role in the observed phenomena.

This work was supported by grant NSH-2170.2003.2 and grants from the Ministry of Science of the Russian Federation.

*E-Mail: gant@issp.ac.ru

[1] D. Jérome and H. J. Schulz, Adv. Phys. **31**, 299 (1982); *ibid.* **51**, 293 (2002).
[2] F. P. Millkén, C. P. Umbach, and R. A. Webb, Solid State Commun. **7**, 309 (1996).
[3] M. Bockrath, D. H. Cobden, J. Lu, A. G. Rinzler, R. E. Smally, L. Balents, and P. L. McEuen, Nature (London) **397**, 598 (1999).
[4] J. L. Costa-Krämer, N. Garsia, P. Garsia-Mochales, and P. A. Serena, Surf. Sci. **342**, L1144 (1995).
[5] R. E. Peierls, *Quantum Theory of Solids*, Clarendon Press, Oxford (1955) [Russian translation, Izd. Inostr. Lit., Moscow (1956)].
[6] V. L. Berezinskiĭ, Zh. Éksp. Teor. Fiz. **65**, 1251 (1973) [JETP **38**, 620 (1973)].
[7] M. Büttiker, Adv. Solid State Phys. **30**, 40 (1990).
[8] Yu. V. Sharvin, Zh. Éksp. Teor. Fiz. **48**, 984 (1965) [JETP **21**, 655 (1965)].
[9] B. J. van Wees, L. P. Kouwenhoven, H. van Houten, C. W. J. Beenakker, J. E. Mooij, C. T. Foxon, and J. J. Harris, Phys. Rev. B **36**, 3625 (1988).
[10] R. Landauer, Philos. Mag. **21**, 863 (1970).
[11] Y. Imry, *Introduction to Mesoscopic Physics*, Oxford University Press (2002).
[12] P. W. Anderson, D. J. Thouless, E. Abrahams, and D. S. Fisher, Phys. Rev. B **22**, 3519 (1980).
[13] A. B. Fowler, A. Harstein, and R. A. Webb, Phys. Rev. Lett. **48**, 196 (1982).
[14] M. Ya. Azbel, Solid State Commun. **45**, 527 (1983).
[15] D. H. Dunlap, H.-L. Wu, and P. W. Phillips, Phys. Rev. Lett. **65**, 88 (1990).
[16] H.-J. Stöckmann, *Quantum Chaos (An Introduction)*, Cambridge University Press (1999) [Russian translation, Fizmatgiz, Moscow (2004)].
[17] F. M. Izrailev and A. A. Krokhin, Phys. Rev. Lett. **82**, 4062 (1999).
[18] F. M. Izrailev and N. M. Makarov, Opt. Lett. **26**, 1604 (2001).
[19] U. Kuhl, F. M. Izrailev, A. A. Krokhin, and H.-J. Stöckmann, Appl. Phys. Lett. **77**, 633 (2000).

Translated by M. E. Alferieff